Frequency-dependent angular scattering of ultrasound by tissue-mimicking materials and excised tissue

W. J. Davros, J. A. Zagzebski, and E. L. Madsen
University of Wisconsin, Department of Medical Physics, Room 1530 MSC, 1300 University Avenue, Madison, Wisconsin 53706

(Received 18 December 1985; accepted for publication 26 March 1986)

An apparatus and method of experimentation for measuring frequency-dependent angle scattering from *in vitro* tissue samples and tissue-like scattering media have been developed. Distinguishing features of this method are that data collection is rapid, data reduction is simple, and results, given in the form of the differential scattering cross section per unit volume, are accurate and absolute. Reported are the results of tests to determine the overall accuracy of the method. Also, results of the differential scattering cross section per unit volume from female human breast tissue are presented.

PACS numbers: 43.35.Yb, 43.80.Cs, 43.80.Qf

INTRODUCTION

In clinical ultrasonic *B*-mode imaging, scattering of sound by tissues plays an important role in visualizing normal and abnormal structures. Current diagnostic ultrasound studies involve transmitting brief pulses of ultrasonic energy into the body and detecting and displaying signals due to acoustic scattering by soft tissues. In most cases only waves scattered back towards the sound source are detected because the same transducer serves as both transmitter and receiver. Gray scale *B*-mode images are formed by intensity modulating a display according to the amplitude of the scattered signals.

Although ultrasonic scattering is largely responsible for characteristics found in clinical ultrasound images, knowledge of the scattering properties of soft tissues and of the exact scattering sites is still sparse. At present, clinical images fail to provide quantitative information on scattering properties because instrument related factors, operator dependencies, and pulse propagation in tissue all have a substantial effect on the signal obtained. Measurements of the *intrinsic* ultrasonic scattering properties of human tissue parenchyma, underway in a number of laboratories, may lead to more accurate diagnosis and more specific tissue differentiation than is currently available in clinical images.[1–6] In addition, a catalog of the scattering properties of human tissues would be useful in the construction of phantoms containing tissue-mimicking materials. These phantoms could be used for testing or as an aid to designing ultrasound imaging instruments.

Complete description of the intrinsic scattering properties of soft tissues requires measurements of both frequency-dependent and angle-dependent scattering. Up until now, scattering as a function of angle has been studied by only a few workers. Shung *et al.* have measured frequency-dependent angle scattering from a dilute suspension of red blood cells and compared their results to relative theoretical predictions.[7] Good agreement between their experimental results and theoretical results was observed. Campbell and Waag have measured frequency-dependent angle scattering of ultrasound by calf liver.[8] They developed a normalization method to obtain absolute average differential scattering cross sections for tissues.[9] Qualitative correlations were made between collagen-containing structures and variations of the scatter amplitude as a function of angle.[10] Other related work by Campbell and Waag includes measuring the contribution to attenuation due to scattering and simulating different liver morphologies through the use of random media with varying structural properties.[11]

Frequency-dependent ultrasonic scattering as a function of angle was measured earlier in this laboratory by Burke.[12,13] This method involved insonifying, with nearly monofrequency tone bursts, a spherical sample, 19 mm in diameter, positioned well into the farfield of an unfocused transmitting transducer. The differential scattering cross section per unit volume was obtained from the ratio of the scattered intensity to the incident intensity using a straightforward data reduction technique. It was shown that the contribution to the total scattered power from coherent scattering from the surface of the sample was negligible compared to the power scattered due to incoherent scattering. Also, quantitatively accurate results were obtained for the case of a discrete spherical target whose diameter was 635 μm and whose physical properties were known.[12] In addition, preliminary results were obtained on scattering for human and other mammalian tissues.

In the work reported here ultrasonic scattering from human breast tissue and tissue-mimicking materials is measured as a function of scattering angle and frequency. The technique described in this paper is essentially the same used by Burke; however, the apparatus and data acquisition scheme have been improved and more extensive tests using phantoms have been carried out. The improved apparatus is capable of rapid data acquisition, thereby minimizing effects of tissue decay that could alter the results of scatter measurements.[12,14] A significant advantage of the technique to be described is that it provides results on intrinsic scattering properties of tissues, while utilizing a simple method of data reduction.

This paper has two goals. The first is to describe the

 0001-4966/86/070229-09$00.80

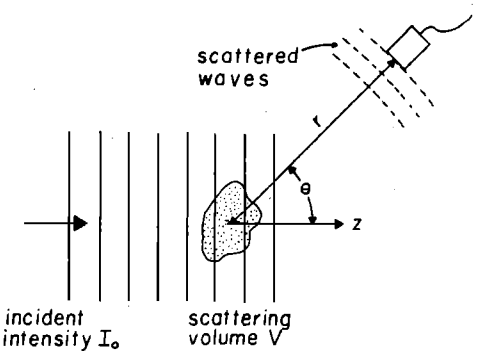

FIG. 1. Schematic representation of a generalized scattering experiment. Shown above are a scattering volume and receiving transducer. The angle θ is defined as the scattering angle and is the angle between the positive z axis and the receiver's beam axis. The distance r is measured from the center of the scattering volume to the face of the receiver. Incident wave fronts are represented by the vertical parallel lines and are defined to have an intensity I_0.

apparatus and experimental methods for rapid measurements of frequency-dependent angular scattering from tissue and tissue-like media. The second goal is to report on quantitative tests of the measurement technique. Also, preliminary results of absolute measurements done on *in vitro* female human breast tissue samples will be presented.

I. THE DIFFERENTIAL SCATTERING CROSS SECTION PER UNIT VOLUME

The differential scattering cross section is generally used for specifying quantitatively the scattering properties of materials including the dependence on the direction of propagation of the scattered waves relative to the direction of propagation of the incident primary beam.[15] Let plane acoustic waves having frequency f and traveling in the $+z$ direction be incident on a scattering region whose volume is V (Fig. 1). If a spherical polar coordinate system is employed and if the scatterers are all close to the origin, compared to the distance to the point of observation, then θ (shown in Fig. 1), and ϕ (the azimuthal angle), identify the direction of scattered waves. The differential scattering cross section, $d\Sigma/d\Omega$, is defined as

$$\frac{d\Sigma}{d\Omega} \equiv \frac{P_\Omega(\theta,\phi)}{I_0}, \tag{1}$$

where $P_\Omega(\theta,\phi)$ is the acoustic power scattered per unit solid angle in the direction (θ,ϕ) and I_0 is the incident wave intensity.

The power scattered is not by itself an intrinsic property of the material since it depends on the volume V. However, if coherent scattering is not significant and if the scatterers are macroscopically homogeneously distributed over V, then the quantity $(1/V)(d\Sigma/d\Omega)$ is independent of V. The differential scattering cross section per unit volume is represented by $(1/V)(d\Sigma/d\Omega)$, and under the above conditions, it is an *intrinsic* property of the scattering material.

Coherent scattering of ultrasound waves could result from two phenomena. First, if the scattering volume is bounded, either due to physical boundaries or to the time-gating of scattered signals, coherent effects associated with these boundaries are present.[1] When measuring scattering from tissues and tissue-mimicking materials, it is necessary to assure that this type of surface coherent scattering is negligible or can be properly accounted for computationally.[12] Second, a volumetric coherent effect might be present, due, for example, to spatial ordering or to dense packing of discrete scatterers.[7,16] However, in general, macroscopically homogeneous volumes of tissue parenchymae are assumed to exhibit little volumetric coherent scattering. Previous studies,[12] as well as data presented in this report, indicate the same is true for tissue-mimicking materials studied in this laboratory.[18] Thus the differential scattering cross section per unit volume is assumed to be an intrinsic property of materials of interest in this report.

In Fig. 1, the scattered intensity is given by $I_s(r,\theta,\phi)$, where r is the distance to the center of the scattering volume; r is assumed to be much greater than the dimensions of V. Since $I_s(r,\theta,\phi)$ is essentially independent of the azimuthal angle ϕ, we will write it as $I_s(r,\theta)$ from here on. If the scattered wave intensity is measured by a detector whose area is A and if $A \ll r^2$, the solid angle it subtends may be approximated by A/r^2. Then, for the differential scattering cross section per unit volume, $\sigma(\theta)$, we have

$$\sigma(\theta) \equiv \frac{1}{V}\frac{d\Sigma}{d\Omega} = \frac{r^2 I_s(r,\theta)}{V I_0}. \tag{2}$$

Thus $\sigma(\theta)$ has dimensions $(\text{length})^{-1}$ $(\text{solid angle})^{-1}$.

One aspect of the incoherently scattered waves has been omitted from the above discussion. Incoherent scattering involves fluctuations in intensity with changes in orientation of the volume containing the scatterers.[17] For incoherent scattering it is the mean value of the scattered intensity $\overline{I}_s$ which is proportional to the volume. Suppose this mean intensity is determined by averaging over N orientations of the sample volume and $I_i(r,\theta)$ refers to the scattered intensity for the ith orientation. Then the expression for the differential scattering cross section per unit volume should be corrected to read

$$\sigma(\theta) = \frac{r^2}{V}\frac{\overline{I}_s(r,\theta)}{I_0} \tag{3}$$

or

$$\sigma(\theta) = \frac{r^2}{VNI_0}\sum_{i=1}^{N} I_i(r,\theta). \tag{4}$$

It is this quantity which is determined experimentally.

II. METHOD OF MEASUREMENT

The measurement apparatus, depicted schematically in Fig. 2, is intended to enable rapid data acquisition as well as a high degree of reproducibility while conforming as closely as possible to assumptions made in the definition of $\sigma(\theta)$. All experiments are conducted in a semicircular water tank that has a radius of 1.2 m and a depth of 25 cm. The water was maintained at a temperature of 22 °C plus or minus one-half of a degree by insulating exposed surfaces of the tank and by using a constant temperature heater/refrigerator unit.

Five matched narrow-band, unfocused transducer pairs (KB Aerotech Delta Series) are used as sources and receiv-

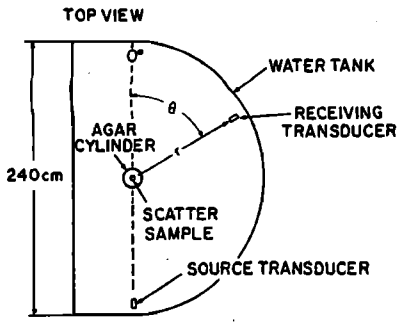

FIG. 2. Top view diagram of the experimental apparatus.

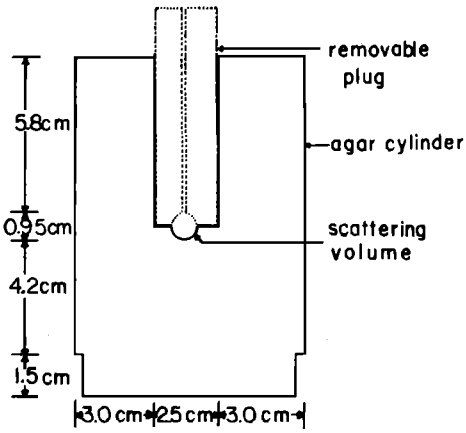

FIG. 3. A crosscut side view of a sample holder cylinder. This drawing is the plan for a 0.95-cm-diam spherical target holder.

ers. These transducers cover the frequency range of 2–10 MHz. The characteristics of each transducer are summarized in Table I. Each source transducer is placed 60 cm from the center of the scattering target and is supported by a mount that permits the transducer to be rotated in both a horizontal and a vertical plane. The matched receiving transducer is suspended by a computer-controlled radial arm assembly centered on the target sample's vertical axis. The receiver can be stationed up to 95 cm from the scattering volume; its face can be rotated about a vertical and horizontal axis. The intersection of these axes is located at the center of the receiver's face. A computer-controlled stepper motor positions the receiver at the scattering angle of interest.

The sample holder is designed to hold a soft tissue sample of a well-defined volume without distorting its shape and to isolate the scattering sample from any other materials that might cause unwanted scattering. The sample holder is cast from an agar and water mix in the shape illustrated in Fig. 3. The sample holder is supported by a Lucite cup that is directly connected to a second computer-controlled stepper motor, allowing the sample to be rotated during data gathering.

The source transducer is driven using a waveform generator (Wavetek model 191) and a power amplifier (ENI model 240L/15P). Typically, the waveform generator is set to produce nearly monofrequency tone bursts approximately 40 μs in duration at a burst rate of 100 Hz.

Signals from the receiver transducer pass through a variable attenuator (Kay model 432D) and are routed to a tuned preamplifier (Matec model 252) and a tuned receiver amplifier (Matec model 605). A segment of the envelope detected output signal from the receiver amplifier is selected by delayed triggering and digitized with a 12-bit, 32-kHz analog-to-digital converter (ADAC model 1012). To avoid contamination from the scattering sphere-to-agar interface, the segment selected is in the middle of the waveform originating from the scattering target as seen in Fig. 4.

Considerable flexibility exists in the choice of experimental parameters that can be used during data acquisition. For 180 orientations of the target per receiver position and using a total of 26 receiver positions, data acquisition takes approximately 20 min. Parameters that are user-selectable include the initial and final receiver-arm angle, the angular increment between successive receiver arm positions, the number of orientations of the target volume per receiver-arm position, and the angular increment between successive target volume orientations. On termination of the master control program for data acquisition, raw data, in the form of analog-to-digital converter numbers, are written to a data file that is stored on a hard disk.

TABLE I. Column 1 lists the center frequency in MHz of each transducer. Column 2 indicates whether each transducer is used as a receiver (R) or a source (S). Column 3 lists the diameter of each transducer's face.

Frequency (MHz)	S/R	Diameter (cm)
2.25	S	2.540
2.25	R	0.635
3.50	S	1.905
3.50	R	0.635
5.00	S	1.270
5.00	R	0.635
7.00	S	1.270
7.00	R	0.635
10.0	S	0.635
10.0	R	0.635

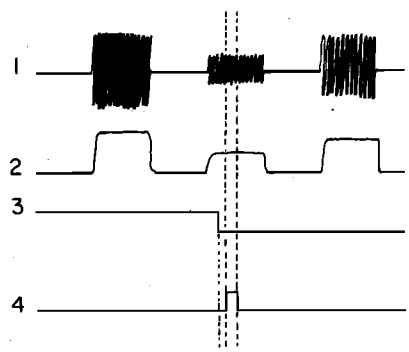

FIG. 4. Timing diagram for the angle scattering experiment. Trace number 1 represents the radio-frequency output of the receiver amplifier as a function of time. Shown are scattered signals originating from the proximal wall of the sample holder, the sample itself, and the distal wall of the sample holder. Trace 2 represents the envelope of trace 1 after rectification. Trace 3 represents a time line from the output of the delayed trigger generator. The analog-to-digital converter is activated 5 μs after the falling edge of the delayed trigger output. Trace 4 represents the activation time of the analog-to-digital converter, shown schematically by a rectangular pulse in the time line. The analog to digital converter is actively connected to the envelope detected signal (trace 2) for 5 μs.

III. CALIBRATION OF THE EQUIPMENT

Calibration of the equipment is a straightforward process. Because the diameter of each of the receiving transducers and the diameter of the scattering volume are small compared to the distance from the scattering target to the face of the receiving transducer, it can be shown that phase cancellation is negligible at the face of the receiving transducer for target diameters equal to or less than 1.9 cm. It is assumed that each receiving transducer converts acoustic pressure to induced voltage in a linear fashion; that is,

$$A_i = kS_i(\theta), \tag{5}$$

where A_i is the amplitude of the received scattered wave, S_i is the resultant induced-voltage amplitude from the receiving transducer, and k is a proportionality constant unique to each receiver. Each value of i corresponds to one of N angular orientations of the target volume, all other parameters, including θ, being held fixed.

The actual process of calibrating the system involves aiming the receiving transducer directly towards the source transducer's face and separating them by a distance equal to the distance between the source and the center of the scattering volume. This arrangement of transducers corresponds to the position where the incident acoustic intensity I_0 must be determined in order to calculate the differential scattering cross section per unit volume. As in the case of the scattered pressure waves, the conversion of the incident acoustic pressure to induced voltage done by the receiving transducer can be expressed using an equation with the same form as Eq. (5), but substituting A_0 for A_i and S_0 for S_i. Thus the ratio of the scattered-to-incident wave amplitudes is equal to the ratio of the corresponding signal amplitudes at the receiving transducer,

$$\frac{A_i}{A_0} = \frac{S_i}{S_0}. \tag{6}$$

To account for attenuation caused by the presence of the agar target-holder cylinder, a uniform agar cylinder is placed between the source transducer and the receiving transducer. The variable attenuator is then adjusted so that the peak-to-peak voltage at the input to the receiver amplifier is within acceptable limits of that device and the delayed trigger is adjusted so that the signal at the receiving transducer is digitized. A calibration data table of analog-to-digital converter numbers versus ratios of scattered signal voltage amplitude to incident signal voltage amplitude is created by varying the setting on the attenuator. The calibration data are fit to a third-order polynomial whose coefficients are used later in the data reduction scheme.

IV. DATA ANALYSIS

The data analysis scheme can be broken down into two steps. The first step entails calculating a correction factor that accounts for attenuation within the scattering volume and for any known nonuniformity of the intensity of the incident ultrasonic beam. The correction factor C is dependent on the scattering sample radius a, the attenuation coefficient of the sample α, the relative intensity beam profile of the incident beam $I(x, y)$, and the scattering angle θ. Here

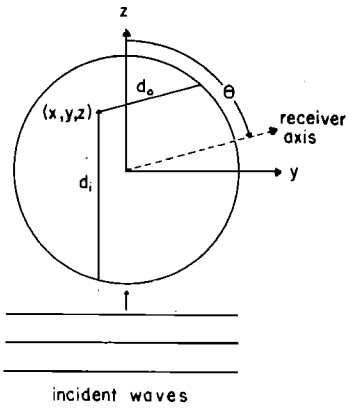

FIG. 5. A top view of the scattering volume illustrating factors used to correct for attenuation within the scattering volume. The parameter d_i represents the distance an incoming wave must travel before it scatters off of a particle located position (x,y,z) and d_0 is the distance a scattered wave must travel before exiting the scattering volume. Both d_i and d_0 are either contained in or parallel to the y–z plane. The angle θ is the scattering angle.

$I(x, y)$ was determined with a hydrophone and the data were normalized to unity at $x = 0$, $y = 0$. The correction factor C is computed using Eq. (7)

$$C = \int_{-a}^{a}\int_{-a}^{a} I(x,y) \int_{-a}^{a} e^{-\alpha(d_0 + d_i)}\, dz\, dy\, dx \times (4\pi a^3/3)^{-1}, \tag{7}$$

where $d_i = z + (a^2 - x^2 - y^2)^{0.5}$,

$$d_0 = -z\cos(\theta) + y\sin(\theta) + [a^2 - x^2 - (y\cos\theta + z\sin\theta)^2]^{0.5},$$

and $dz\,dy\,dx$ represents a volume element. Only points (x, y, z) such that $x^2 + y^2 + z^2 < a^2$ are included in the calculation of C.

The distance the incident wave must travel within the spherical sample before it interacts with a scatterer located at Cartesian coordinates (x, y, z) is d_i; the direction of travel is parallel to the beam axis of the source transducer. The distance the scattered wave must travel before exiting the spherical sample is d_0; the direction of travel is parallel to the receiving transducer's "beam axis." These two distances are illustrated in Fig. 5.

Using Eq. (6), and recalling the relationship between acoustic pressure (A) and intensity (I), the differential scattering cross section per unit volume $\sigma(\theta)$ can be expressed as

$$\sigma(\theta) = \frac{e^{\alpha_w r} r^2}{NCV} \sum_{i=1}^{N} \left(\frac{S_i}{S_0}\right)^2, \tag{8}$$

where $e^{\alpha_w r}$ accounts for attenuation in the water path from the target cylinder holder surface to the receiving transducer face, α_w being the attenuation coefficient of water.

V. PREPARATION OF TISSUE-LIKE TARGETS

Two well-characterized scattering targets were constructed for the purpose of testing the accuracy of the apparatus and data reduction method. These targets consist of microscopic solid glass beads that are spatially randomly distributed in a scatter-free gel.[18,19] The targets were cast

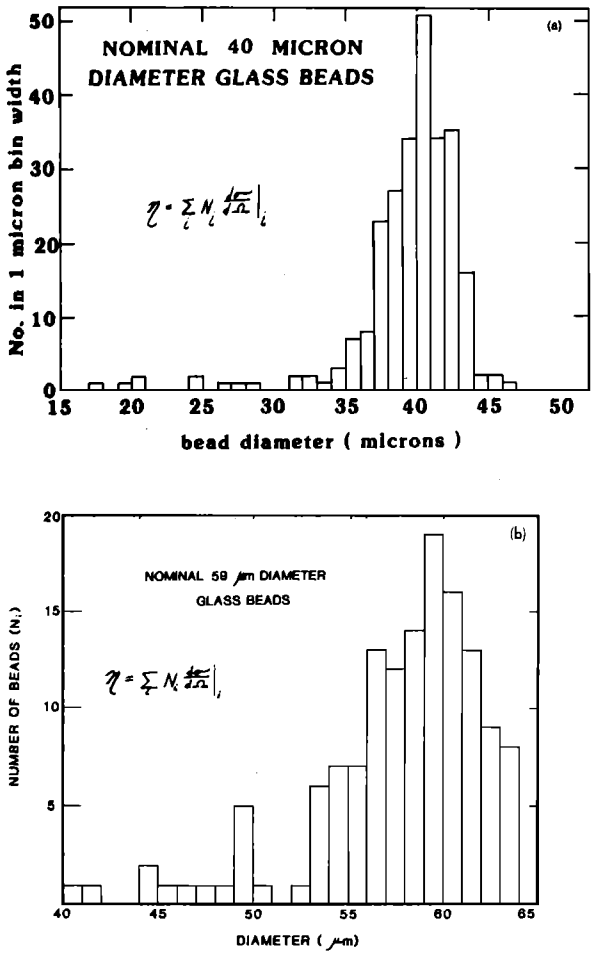

FIG. 6. Histogram of the diameter distribution of glass beads having a nominal diameter of (a) 40 μm and (b) 58 μm. The bin width for each histogram is 1 μm.

into 1.9-cm-diam spheres. Each spherical target is imbedded in its own scatter-free agar cylinder. The speed of sound of these targets is 1500 m/s and the density of the targets is 1.0 g/cm^3.

Theoretical predictions of the differential scattering cross section per unit volume were calculated using expressions derived by Faran.[20] These expressions predict the scattered pressure from a single solid sphere insonified by plane waves. The asymptotic form of the equation used to calculate the scattered pressure[20] was used to compute the ratio of the scattered-to-incident intensity; this is valid in the present study since the distance to the point of observation is much greater than the diameter of the sphere doing the scattering. Since the scatterers are spatially randomly distributed and the mean distance between scatterers is large compared to the diameter of a scatterer, the differential scattering cross section for the target is taken as n times the differential scattering cross section per scatterer, where n is the total number of scatterers in the sphere.

To utilize Faran's theory, the longitudinal wave speed of sound, density, and Poisson's ratio must be known for the glass beads. These quantities were specified by the manufacturer of the glass beads (Potters Industries, Hasbrouck, New Jersey). Also, the glass bead diameter distributions for each of the samples must be known; these were determined optically. This entailed taking a thin slab of each of the target materials and measuring bead diameters using a calibrated microscope with a movable vernier scale eyepiece. Several hundred beads from each target sample were sized and grouped into size bins, each bin consisting of a narrow range of diameters. Figure 6(a) and (b) represents the diameter distributions of the glass beads used. To compute the theoretical differential scattering cross section it was assumed that all beads in any given bin were of one diameter, that being the mean diameter of that particular bin. For the material shown in Fig. 6(a), there are 39 beads/mm^3 and for the material shown in Fig. 6(b) there are 7.7 beads/mm^3.

To test the method's ability to adequately account for attenuation in the scattering volume, two other samples were constructed. As before, these samples, consisted of solid glass beads spatially randomly distributed in a scatter-free gel. Each target was cast into a 1.27-cm-diam sphere and each was embedded in its own scatter-free agar cylinder. Both samples contained exactly the same concentration and diameter distribution of glass beads and therefore were assumed to have the same scattering strength. These two samples differed only in their attenuation coefficient, one being low attenuation (0.13 ± 0.04 dB cm^{-1}MHz^{-1}) and the other having tissue-like attenuation (0.64 ± 0.01 dB cm^{-1} MHz^{-1}) through the addition of 60 g/liter of graphite powder.[18] The graphite powder is fine grain and yields negligible scattering by itself. Attenuation coefficients were measured using a narrow-band substitution technique.[21]

VI. HUMAN TISSUE HANDLING

Female human breast tissue samples used in this study were obtained from surgical breast reduction procedures. Once a breast tissue sample has been removed from a patient it is placed in an airtight container and refrigerated until it is delivered from the University of Wisconsin Hospital to the ultrasound laboratory, approximately 2 miles away. Typically, tissue is no more than 3 h old before it is delivered to the ultrasound lab. When tissue is received, it is examined visually to locate a region approximately 0.5 cm^3 in volume that is free of large fat globules. When such a region is located it is removed from the bulk sample, carved into a roughly spherical shape, and loaded under water into a sample holder cylinder illustrated in Fig. 3. At the conclusion of any experiments performed on tissue samples, the sample's density and mass are measured and its volume is calculated. In addition, the attenuation coefficient of the bulk sample is measured using a narrow-band substitution technique.[21]

VII. RESULTS AND DISCUSSION

The data illustrated in Fig. 7 are results from experiments to test the overall accuracy of the measurement technique. Results are presented for ultrasonic frequencies of 2.5, 3.0, 3.5, 4.0, 6.0, and 7.0 MHz. In each case the attenuation coefficient of the target was identical to the attenuation coefficient of the uniform agar cylinder used in the calibration procedure. Thus the net attenuation coefficient used in the calculation of the correction factor C given by Eq. (7) was zero. In the plots illustrated in Fig. 7, experimental re-

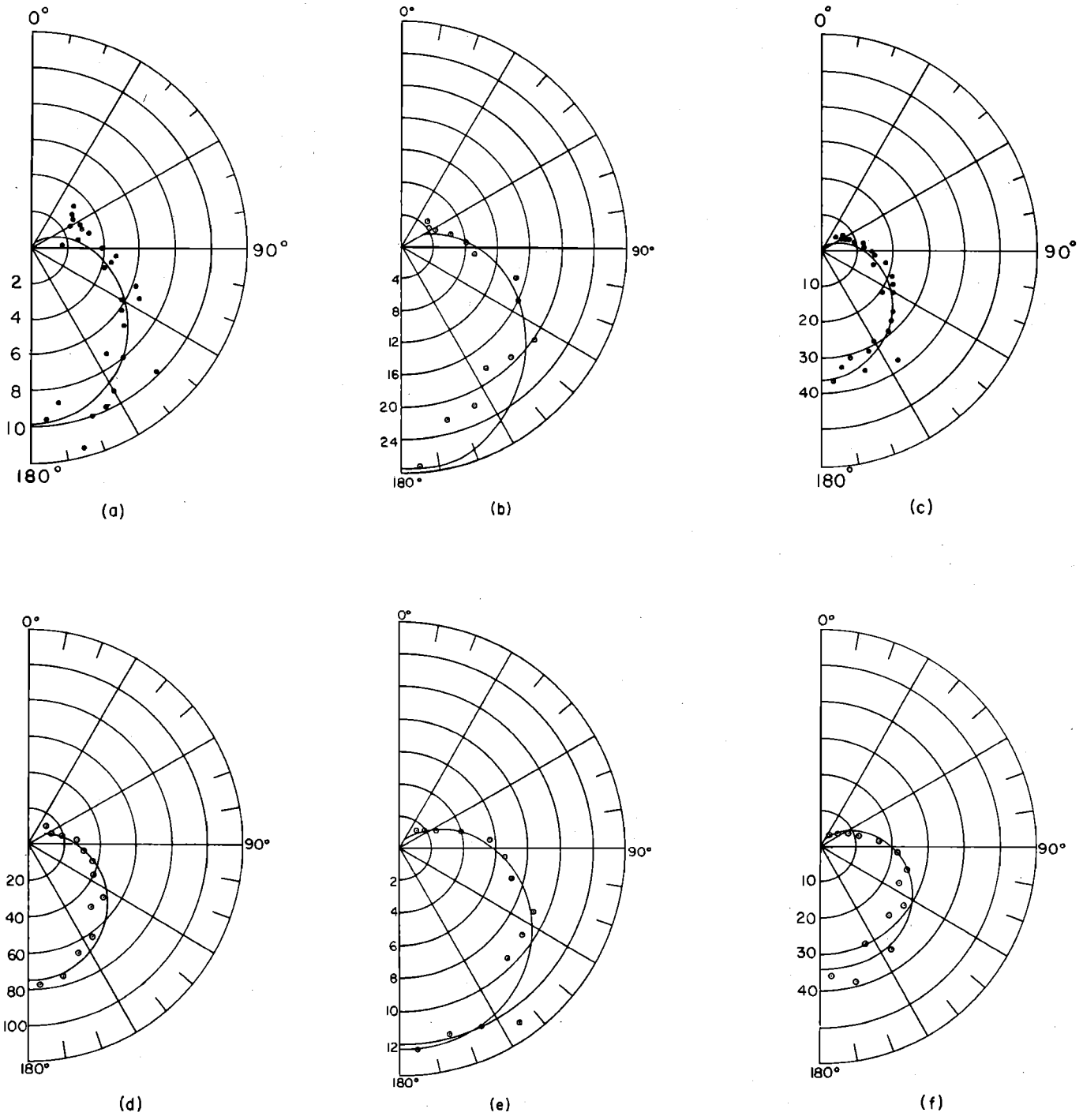

FIG. 7. Experimental (dots) and theoretical (smooth curve) $\sigma(\theta)$ for targets consisting of glass beads in gel. Units for $\sigma(\theta)$ are $cm^{-1}\ sr^{-1}$. (a) Radial increments are times 10^{-5}, the ultrasonic frequency used was 2.25 MHz, and the nominal particle diameter for the distribution is 40 μm. (b) Radial increments are times 10^{-5}, the ultrasonic frequency used was 3.0 MHz, and the nominal particle diameter for the distribution is 58 μm. (c) Radial increments are times 10^{-5}, the ultrasonic frequency used was 3.5 MHz, and the nominal particle diameter for the distribution is 40 μm. (d) Radial increments are times 10^{-5}, the ultrasonic frequency used was 4.0 MHz, and the nominal particle diameter for the distribution is 58 μm. (e) Radial increments are times 10^{-4}, the ultrasonic frequency used was 6.0 MHz, and the nominal particle diameter for the distribution is 58 μm. (f) Radial increments are times 10^{-4}, the ultrasonic frequency used was 7.0 MHz, and the nominal particle diameter for the distribution is 40 μm.

sults are represented by data points and the theoretical prediction is represented by a solid line. It can be seen that for all frequencies investigated, experimental results and theoretical predictions are in excellent agreement for all scattering angles. One possible exception is $\theta < 70°$ and $f < 7.0$ MHz. This could be due to the fact that at frequencies less than 7.0 MHz and scattering angles less than 70°, unwanted signals due to the incident ultrasonic beam are being picked up by the receiver.

The data illustrated in Fig. 8 indicate that the data re-

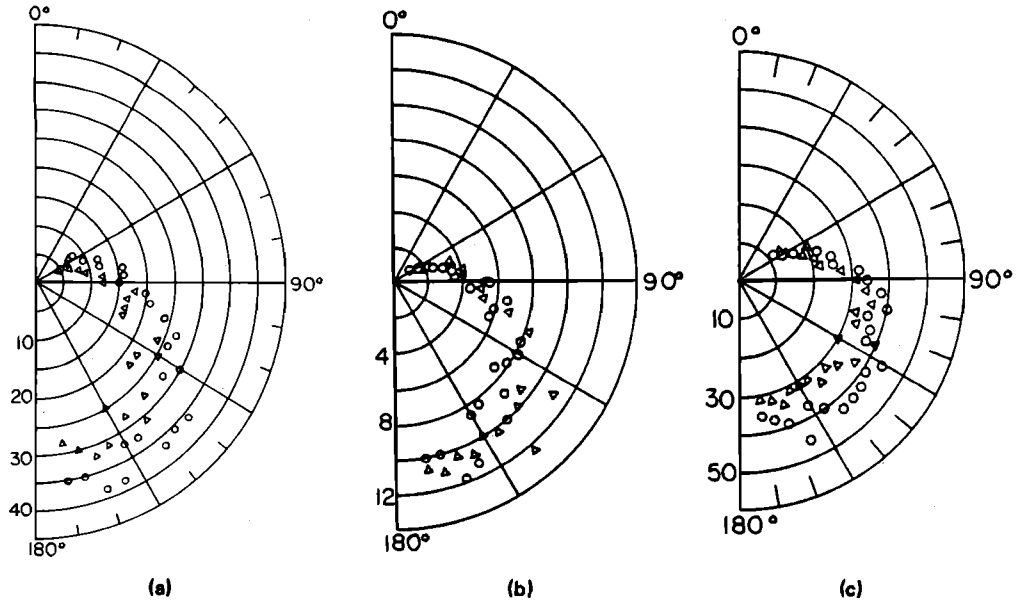

FIG. 8. Experimental $\sigma(\theta)$ for the low attenuation sample are plotted as triangles (Δ) and experimental $\sigma(\theta)$ for the tissue-like attenuation sample are plotted as circles (O). As in Fig. 5, $\sigma(\theta)$ is plotted in units of $cm^{-1}sr^{-1}$. (a) Radial increments are times 10^{-5}, and the ultrasonic frequency used was 2.25 MHz. (b) Radial increments are times 10^{-4}, and the ultrasonic frequency used was 3.5 MHz. (c) Radial increments are times 10^{-4}, and the ultrasonic frequency used was 7.0 MHz.

duction method correctly accounts for attenuation in the scattering volume when the attenuation coefficient is known. In Fig. 8, the triangles represent data collected from the target whose *net* attenuation (attenuation coefficient of the target minus the attenuation coefficient of the calibration cylinder) was 0.0 dB cm^{-1} MHz^{-1}; the solid circles represent data collected from the target whose *net* attenuation coefficient was $0.51 \pm .01$ dB cm^{-1} MHz^{-1} with respect to the calibration cylinder. From Fig. 8 it can be seen that the method of accounting for attenuation in the volume doing scattering appears to be adequate for the ultrasonic frequencies investigated. Any differences noted are most likely due to precision errors in the position of the sample and the alignment of the transducers. The later error could occur either when the receiver signal was being maximized prior to the data collection process or when the receiver signal was being maximized during the calibration procedure.

Preliminary results of $\sigma(\theta)$ have been obtained from samples of female human breast tissue from four individuals. In each of the experiments, scattered echo signals were recorded for 180 unique sample orientations, separated by two degrees for each scattering angle θ. The total time for data collection from one experiment, comprised of 24 scattering angles and 180 sample positions per scattering angle, was 20 min.

Figure 9(a) and (b) shows representative results from these experiments. In each case the tissue was approximately 3 h old and studies were conducted at 3.5 MHz. Figure 10 presents mean data at 3.5 MHz from the breast tissue of four individuals. The error bars shown in Fig. 10 represent plus and minus one standard deviation, centered at the mean value of σ for each value of θ investigated. It is interesting to note that for the breast tissue samples studied thus far, there seems to be little dependence of scattering on θ for scattering angles between 170°–85°. Also, these samples exhibited a significant amount of forward scattering. Similar results on the angular dependence have been observed in other tissues as well.[8]

VIII. SUMMARY AND CONCLUSION

A method has been developed for measuring frequency- and angle-dependent scattering of ultrasound by tissues. Extensive tests of the accuracy of the apparatus and method were done on samples whose physical properties were

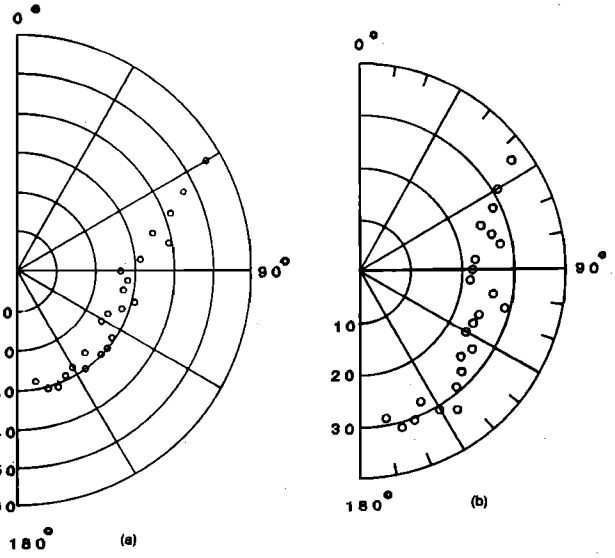

FIG. 9. Experimental results of $\sigma(\theta)$ from female human breast tissue; (a) and (b) are results from the samples of two individuals. Radial increments are times 10^{-4} cm^{-1} sr^{-1} and the ultrasonic frequency used was 3.5 MHz.

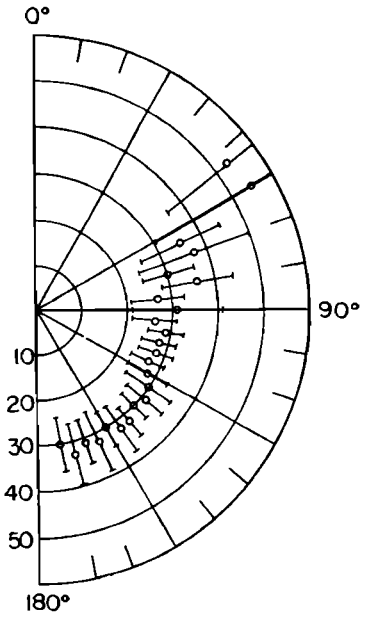

FIG. 10. Plotted is the average $\sigma(\theta)$ from four samples of human breast tissue from four individuals. Error bars represent plus and minus one standard deviation. As before, $\sigma(\theta)$ has units of $cm^{-1}\,sr^{-1}$. Radial increments are times 10^{-4}, and the ultrasonic frequency used was 3.5 MHz.

known and whose scattering characteristics were predicted by theory. In these tests, experimental data were in excellent agreement with theoretical predictions. These tests were conducted over a range of frequencies often used in clinical diagnostic ultrasound imaging. Additional tests, using scattering volumes with identical scattering properties but different attenuation coefficients, demonstrate that the data reduction scheme does adequately account for attenuation in the volume doing the scattering.

Preliminary results of the average differential scattering cross section per unit volume from four samples of human breast tissue, each from a different individual, were presented. Sample-to-sample variability of $\sigma(\theta)$ was small, averaging 20% over the scattering angles at which measurements were taken. For scattering angles from 180°–90°, the average differential scattering cross section per unit volume exhibited very little dependence on θ; for angles less than 90° pronounced forward scattering was noted. Obviously, many more breast tissue samples will need to be measured before definitive conclusions on the angular and frequency dependence of scattering from female human breast tissue can be drawn from experimental data.

The method and apparatus described in this report display promising prospects as a way to measure absolute scattering from small volumes of tissue accurately and rapidly. This technique is capable of rapid data acquisition, thus minimizing unwanted effects due to sample degradation. Currently, this apparatus and technique are being used as a tool in the development of phantom materials having tissue-like scattering, and as a means of acquiring data needed to catalog intrinsic scattering from various tissues.

ACKNOWLEDGMENTS

A number of individuals deserve special mention in connection with the studies reported here. Acknowledged for their contributions and assistance are Gary Frank, Evan Boote, Mike Insana, Tim Hall, Kathy McSherry, and Colleen Schutz. This work was supported in part by National Institutes of Health grants RO1CA25634 and RO1GM30522 (now RO1CA39224).

[1]E. L. Madsen, M. F. Insana, and J. A. Zagzebski, "Method of data reduction of acoustic backscatter coefficients," J. Acoust. Soc. Am. **76**, 913–923 (1984).

[2]D. Nicholas, "Evaluation of backscattering coefficients of excised human tissue: Results, interpretations, and associated measurements," Ultrasound Med. Biol. **8**, 17–28 (1982).

[3]M. F. Insana, J. A. Zagzebski, and E. L. Madsen, "Acoustic backscattering from ultrasonically tissuelike media," Med. Phys. **9**, 848–855 (1982).

[4]K. K. Shung, "An alternative approach for formulating the backscattering equation in Sigelmann and Reid's method," J. Acoust. Soc. Am. **73**, 1384–1386 (1983).

[5]D. Y. Fei and K. K. Shung, "Ultrasonic backscatter from mammalian tissues," J. Acoust. Soc. Am. **78**, 871–876 (1985).

[6]M. O'Donnell, J. W. Mimbs, and J. G. Miller, "Relationship between collagen and ultrasonic backscattering in myocardial tissues," J. Acoust. Soc. Am. **69**, 580–588 (1981).

[7]K. K. Shung, R. A. Sigelmann, and J. M. Reid, "Angular dependence of scattering of ultrasound from blood," IEEE Trans. Biomed. Eng. **BME-24**(4), 325–331 (July 1977).

[8]J. A. Campbell and R. C. Waag, "Measurements of calf liver ultrasonic differential and total scattering cross sections," J. Acoust. Soc. Am. **75**, 603–611 (1984).

[9]J. A. Campbell and R. C. Waag, "Normalization of ultrasonic scattering measurements to obtain average differential scattering cross sections for tissues," J. Acoust. Soc. Am. **74**, 393–399 (1983).

[10]R. C. Waag, P. P. K. Lee, H. W. Persson, E. A. Schenk, and R. Gramiak, "Frequency-dependent angle scattering of ultrasound by liver," J. Acoust. Soc. Am. **72**, 343–352 (1982).

[11]J. A. Campbell and R. C. Waag, "Ultrasonic scattering properties of three random media with implications for tissue characterization," J. Acoust. Soc. Am. **75**, 1879–1886 (1984).

[12]T. M. Burke, "Quantitative characterization of the intrinsic-scatter nature of tissue and tissue-mimicking materials," Ph.D. thesis, Department of Medical Physics, University of Wisconsin–Madison (1982).

[13]T. M. Burke, M. M. Goodsitt, E. L. Madsen, and J. A. Zagzebski, "Angular distribution of scattered ultrasound from a single steel sphere in agar gelatin: A comparison between theory and experiment," Ultrasonic Imaging **6**, 342–347 (1984).

[14]J. C. Bamber, M. J. Fry, C. R. Hill, and F. Dunn, "Ultrasonic attenuation and backscattering by mammalian organs as a function of time after excision," Ultrasound Med. Biol. **3**, 15–20 (1977).

[15]P. M. Morse and K. U. Ingard, *Theoretical Acoustics* (McGraw-Hill, New York, 1968), p. 407.

[16]J. M. Reid, in *Medical Physics of CT and Ultrasound*, edited by G. D. Fullerton and J. A. Zagzebski, American Association of Physicists in Medicine Summer School Proceedings, AAPM Monograph No. 6 (AAPM, New York, 1980), p. 395.

[17]R. F. Wagner, S. W. Smith, J. M. Sandrick, and H. Lopez, "Statistics of speckle in ultrasound B-Scans," IEEE Trans. Sonics Ultrason. **SU-30**, (1983).

[18]E. L. Madsen, J. A. Zagzebski, R. A. Banjavic, and R. E. Jutilla, "Tissue-

mimicking materials for ultrasonic phantoms," Med. Phys. **5**, 391–394 (1978).
[19]E. L. Madsen, J. A. Zagzebski, M. F. Insana, T. M. Burke, and G. R. Frank, "Ultrasonically tissue-mimicking liver including the frequency dependence of backscatter," Med. Phys. **9**, 703–710 (1982).
[20]J. J. Faran, "Sound scattering by solid cylinders and spheres," J. Acoust. Soc. Am. **23**, 405–418 (1951).
[21]E. L. Madsen, J. A. Zagzebski, and G. Frank, "Oil-in-gelatin dispertions for use as ultrasonically tissue mimicking material," Ultrasound Med. Biol. **8**, 277–287 (1982).